RISC maturation

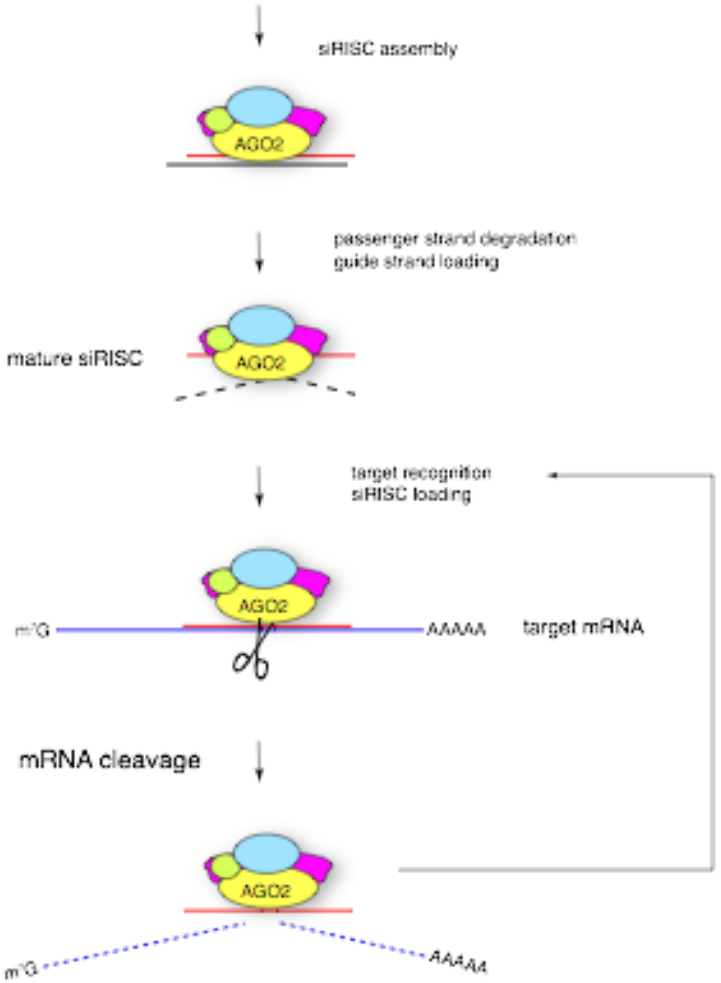

maturazione di RISC: scelta del filamento guida

Cell, Vol. 115, 199–208, October 17, 2003, Copyright ©2003 by Cell Press

Asymmetry in the Assembly of the RNAi Enzyme Complex

Dianne S. Schwarz,[1,3] György Hutvágner,[1,3] Tingting Du,[1] Zuoshang Xu,[1] Neil Aronin,[2] and Phillip D. Zamore[1,*]

[1]Department of Biochemistry and Molecular Pharmacology and

[2]Department of Medicine

University of Massachusetts Medical School

Lazare Research Building

364 Plantation Street

Worcester, Massachusetts 01605

asimmetria nella composizione dei filamenti ss-siRNA caricati su RISC

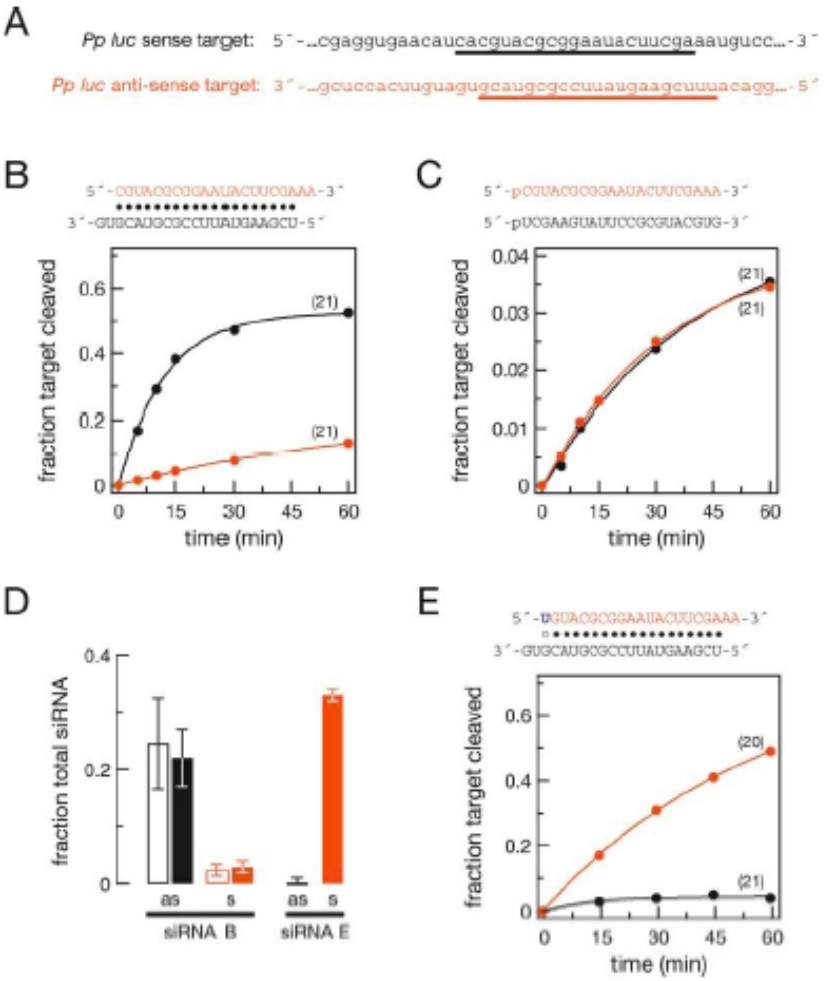

Figure 1. The Two Strands of an siRNA Duplex Do Not Equally Populate the RISC

(A) Firefly luciferase sense and anti-sense target RNA sequences.

(B) In vitro RNAi reactions programmed with the siRNA duplex indicated above the graph.

(C) In vitro RNAi reactions as in (B) but programmed with either the anti-sense or sense single-stranded, 5′ phosphorylated siRNAs indicated above the graph.

(D) Fraction of anti-sense (black) and sense (red) siRNA strands assembled into RISC (open columns) or present as single strands (filled columns) after incubation with *Drosophila* embryo lysate for the siRNA duplexes shown in (B) and (E). The average of four trials ± standard deviation is shown.

(E) In vitro RNAi reactions programmed with the siRNA duplex indicated above the graph and the target RNAs in (A). Throughout the figures, the number of Watson-Crick base pairs formed between the siRNA guide strand and the target RNA is indicated in parentheses, and siRNA bases that mismatch with the target RNA are noted in blue.

un singolo legame idrogeno può determinare la scelta del filamento guida

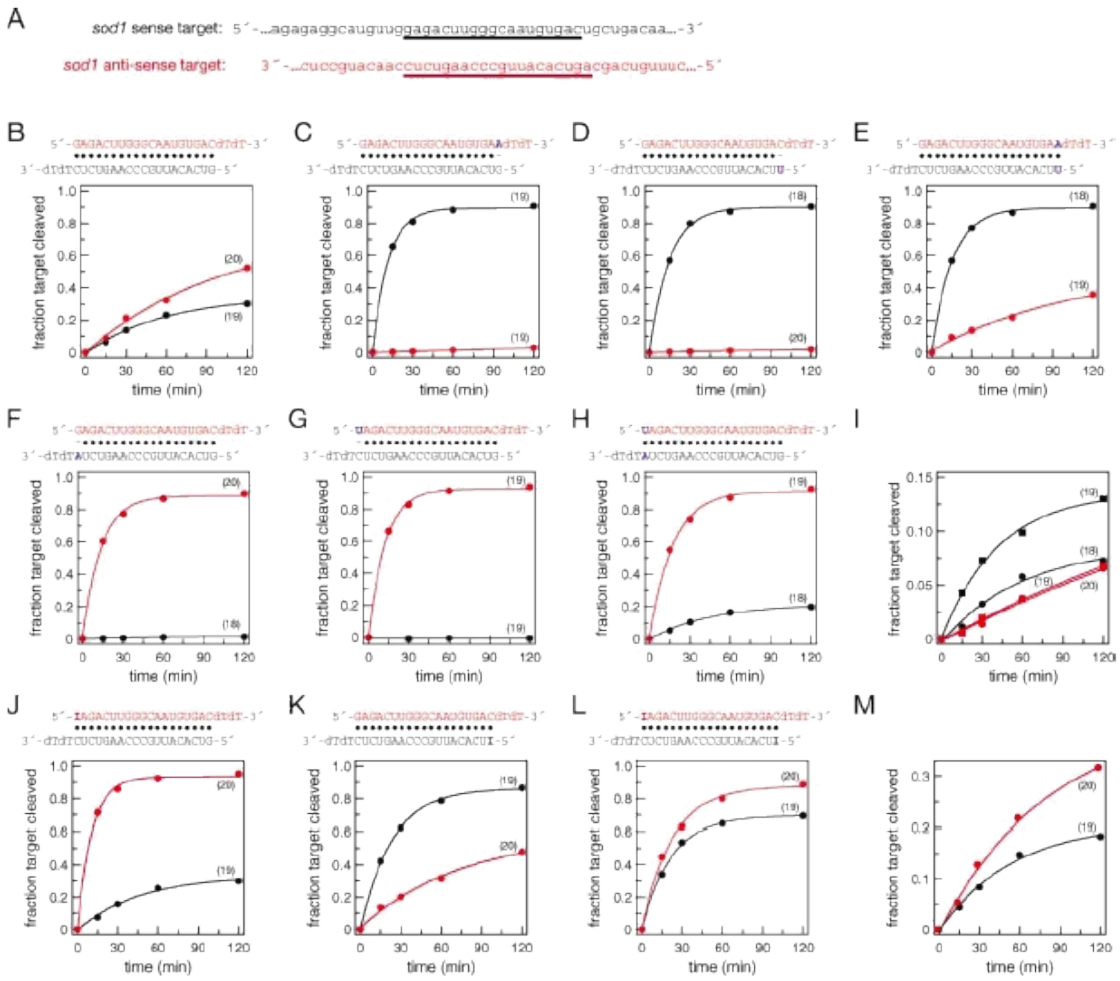

importanza delle prime 4 basi al 5'

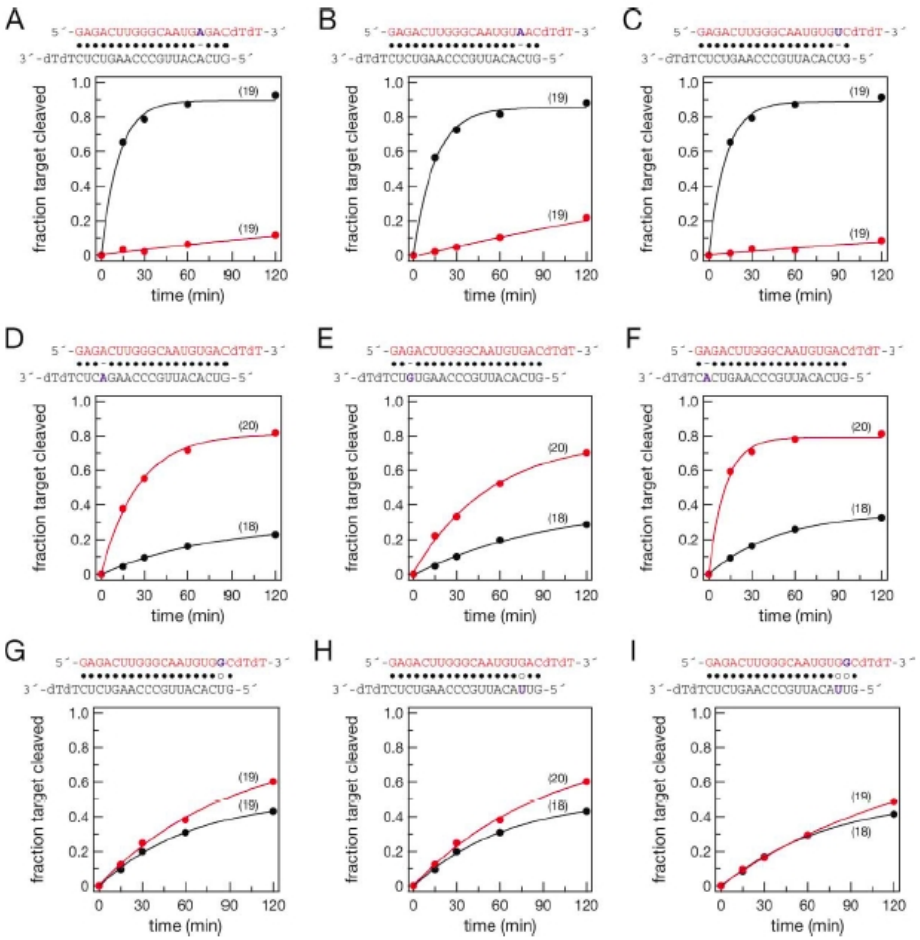

Figure 3. The First Four Base Pairs of the siRNA Duplex Determine Strand-Specific Activity

Internal, single-nucleotide mismatches (A–F) near the 5′ ends of an siRNA strand generate functional asymmetry but internal G:U wobble pairs (G–I) do not. Target RNAs were as in Figure 2A.

modello proposto

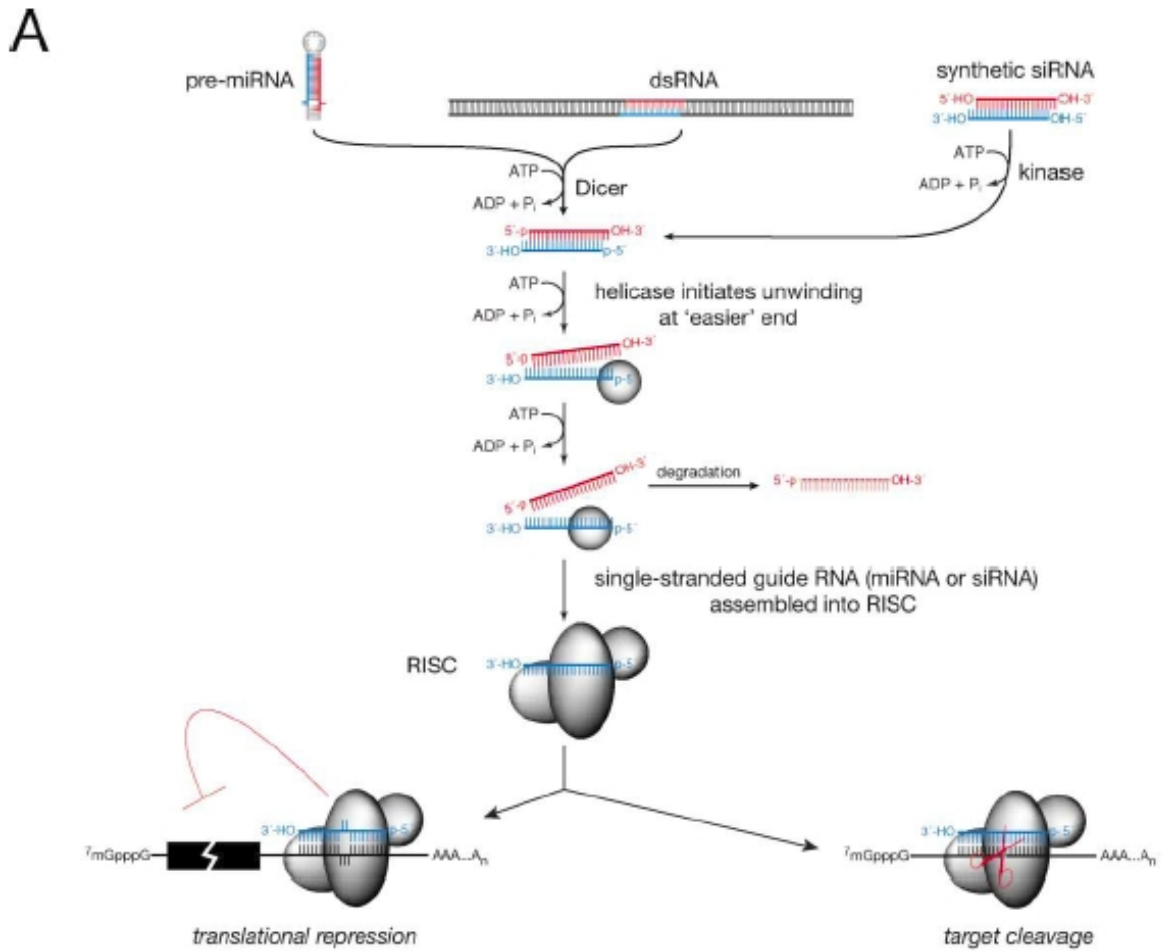

verifica del modello su miRNA caratterizzati di *Drosophila*

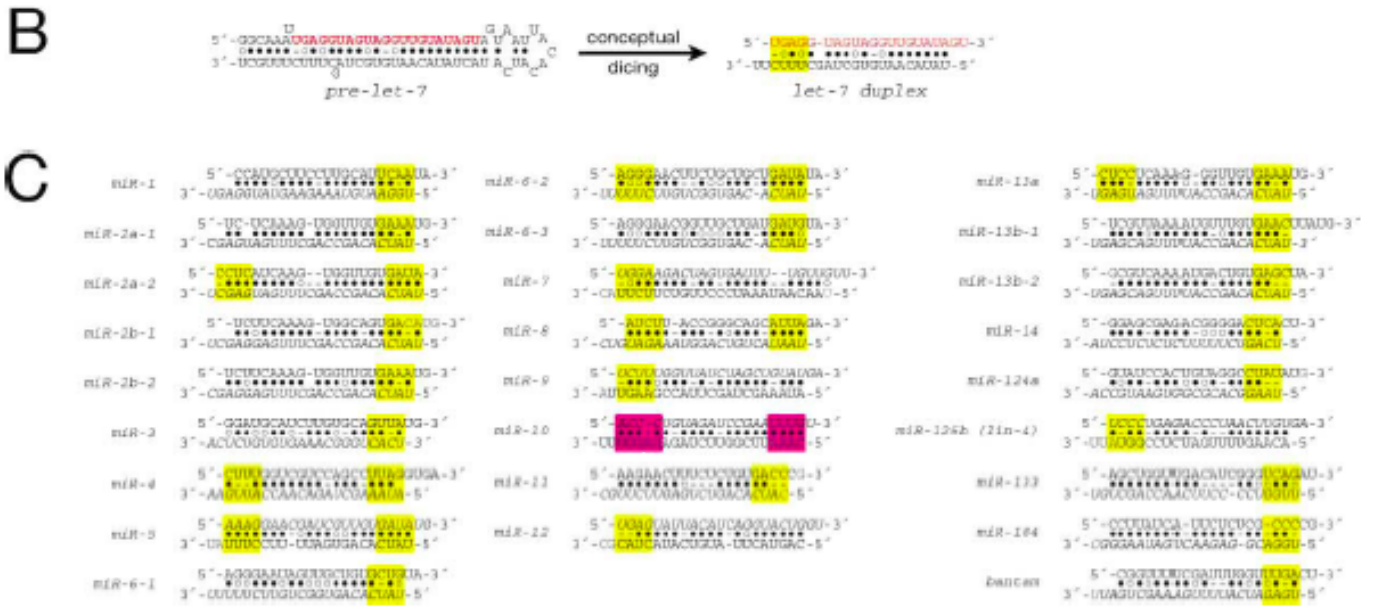

Figure 4. Asymmetric RISC Assembly Can Explain siRNA and miRNA Strand Choice

(A) A model for RISC assembly. Dicing of both pre-miRNAs and dsRNA is proposed to generate a duplex intermediate that is a substrate for an ATP-dependent RNA helicase that directs only one of the two strands into RISC; the other strand is degraded.

(B and C) Asymmetric RISC assembly from double-stranded intermediates explains why miRNAs accumulate in vivo as single strands. (B) pre-*let-7* might be processed by Dicer into a miRNA duplex in which the 5′ end of *let-7*, but not that of *let-7**, is unpaired. (C) The miRNA duplexes predicted to result from Dicer cleavage of *Drosophila* miRNA precursors. The end bearing features predicted to promote asymmetric siRNA strand incorporation into RISC is highlighted in yellow, and the mature miRNA sequence is in italics. Analysis of the predicted miR-10/miR-10* duplex, for which both ends are highlighted in purple, provides little information as to why miR-10 would predominate in vivo. miRNA sequences are from Lagos-Quintana et al. (2001) and Brennecke et al. (2003), with minor sequence corrections from Aravin et al. (2003); miRNA* sequences for miR-2a-2, miR-4, miR-8, miR-10, and miR-13a are as reported by Aravin et al. (2003).

Cell, Vol. 115, 199–208, October 17, 2003, Copyright ©2003 by Cell Press

profili di stabilità termodinamica di siRNA funzionali e non funzionali

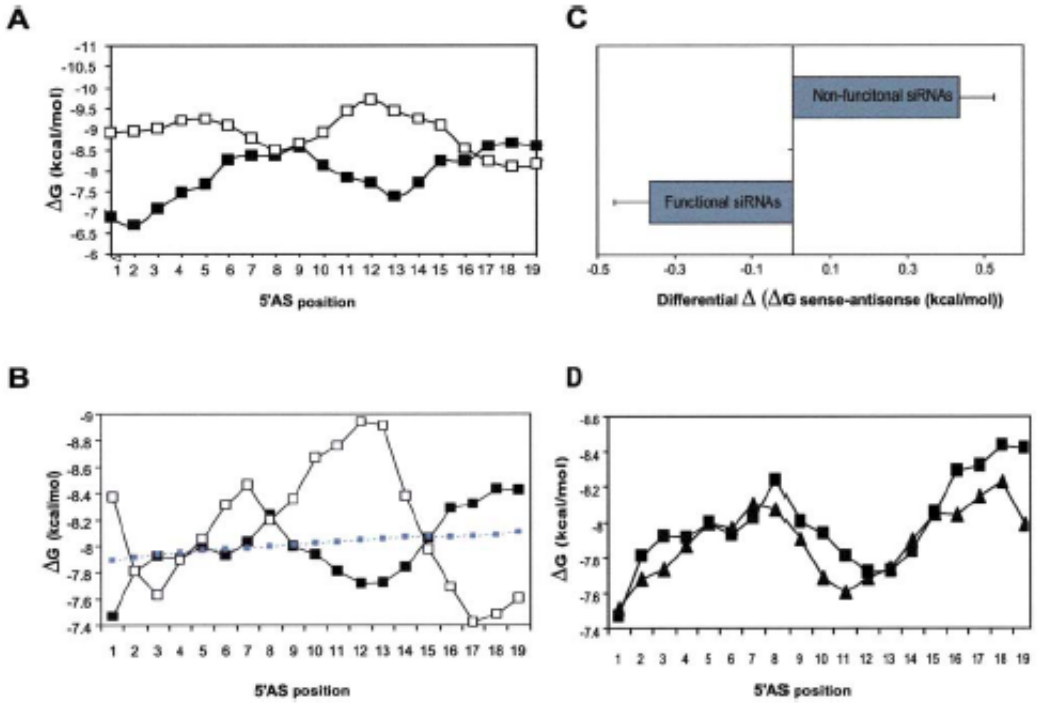

Figure 2. Characterization of the siRNAs Internal Stability Profile

(A) Calculated average internal stability profiles for a set of 37 siRNAs targeting human and mouse genes (functional siRNAs, ■, sample size of 16; and nonfunctional siRNAs, □, sample size of 21).

(B) Calculated average internal stability profiles for a set of 180 siRNAs targeting every other position of firefly luciferase and human cyclophilin (functional siRNAs, ■, sample size of 53; nonfunctional siRNAs, □, sample size of 41; the complete siRNA panel, ■, sample size of 180).

(C) Calculated differential average internal stability of 5′ S and 5′ AS end of 180 siRNA duplexes for functional and nonfunctional subsets (5′ S–5′ AS).

(D) Calculated average internal stability profiles for a set of 59 GFP-related siRNAs identified by cloning after introduction of the long double-stranded GPF RNA into the plant cells (GFP related siRNAs, ▲; functional siRNAs from the 180 siRNA panel, ■).

Cell, Vol. 115, 209–216, October 17, 2003, Copyright ©2003 by Cell Press

identificazione di 'SLICER' in siRISC: il cerchio si chiude su Argonaute!

SCIENCE VOL 305 3 SEPTEMBER 2004

Crystal Structure of Argonaute and Its Implications for RISC Slicer Activity

Ji-Joon Song,[1,2] Stephanie K. Smith,[2] Gregory J. Hannon,[1] Leemor Joshua-Tor[1,2]*

Argonaute2 Is the Catalytic Engine of Mammalian RNAi

Jidong Liu,[1]* Michelle A. Carmell,[1,2]* Fabiola V. Rivas,[1] Carolyn G. Marsden,[1] J. Michael Thomson,[3] Ji-Joon Song,[1] Scott M. Hammond,[3] Leemor Joshua-Tor,[1] Gregory J. Hannon[1]†

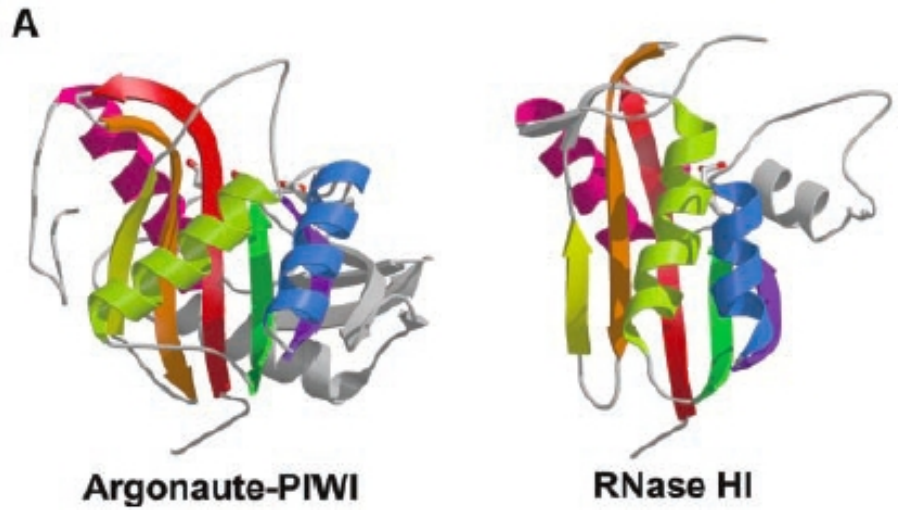

mAgo2 è associata a complessi siRISC competenti per il taglio del mRNA target

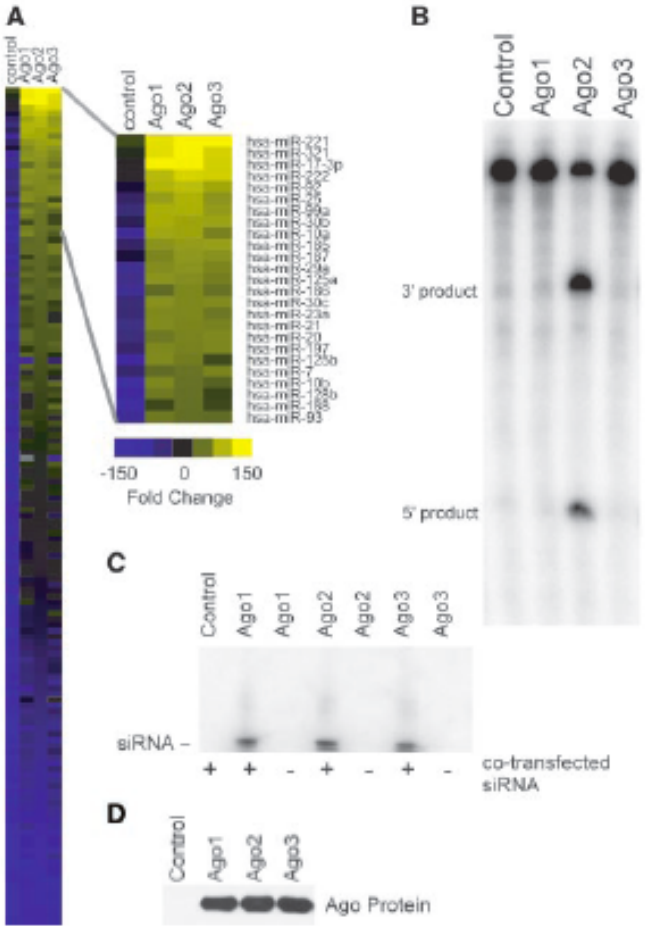

Fig. 1. Only mammalian Ago2 can form cleavage-competent RISC. (**A**) The miRNA populations associated with Ago1, Ago2, and Ago3 were measured by microarray analysis as described in (*44*). The heat map shows normalized log-ratio values for each data set, with yellow representing increased relative amounts and blue indicating decreased amounts relative to the median. The top 25 log ratios are shown in the expanded region. In each panel, "control" indicates parallel analysis of cells transfected with a vector control. (**B**) The 293T cells were transfected with a control vector or with vectors encoding myc-tagged Ago1, Ago2, or Ago3, along with an siRNA that targets firefly luciferase. Immunoprecipitates were tested for siRNA-directed mRNA cleavage as described in (*44*). Positions of 5′ and 3′ cleavage products are shown. (**C**) Immunoprecipitates as in (B) were tested for in vivo siRNA binding by Northern blotting of Ago immunoprecipitates (*44*). (**D**) Western blots of transfected cell lysates show similar levels of expression for each recombinant Argonaute protein.

3 SEPTEMBER 2004 VOL 305 SCIENCE

mAgo2 essenziale per l'interference in fibroblasti embrionali di topo

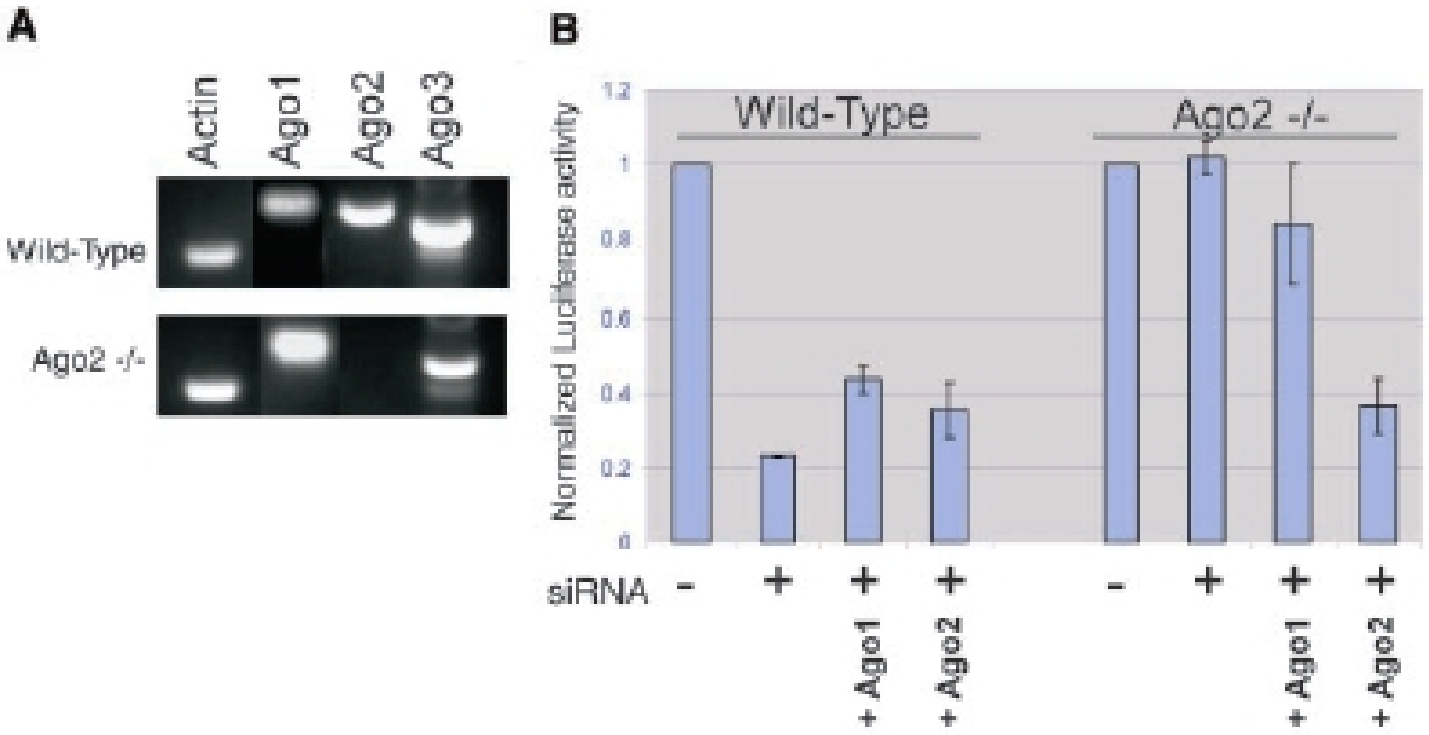

struttura del cristallo di *Pf*Ago

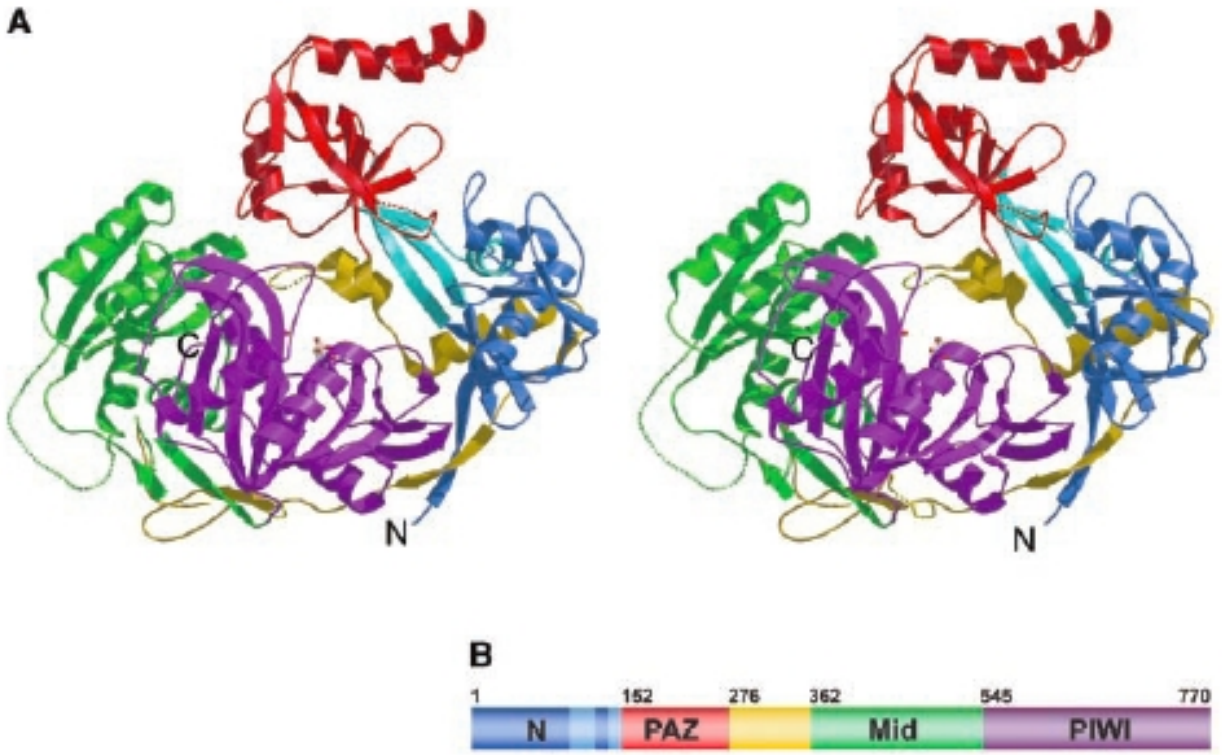

Fig. 1. Crystal structure of *P. furiosus* Argonaute. (**A**) Stereoview ribbon representation of Argonaute showing the N-terminal domain (blue), the "stalk" (light blue), the PAZ domain (red), the middle domain (green), the PIWI domain (purple), and the interdomain connector (yellow). Active site residues are drawn in stick representation. Disordered loops are drawn as dotted lines. (**B**) Schematic diagram of the domain borders.

3 SEPTEMBER 2004 VOL 305 SCIENCE

PAZ domain: sovrapposizione delle strutture *Pf*Ago e *Hs*Ago1

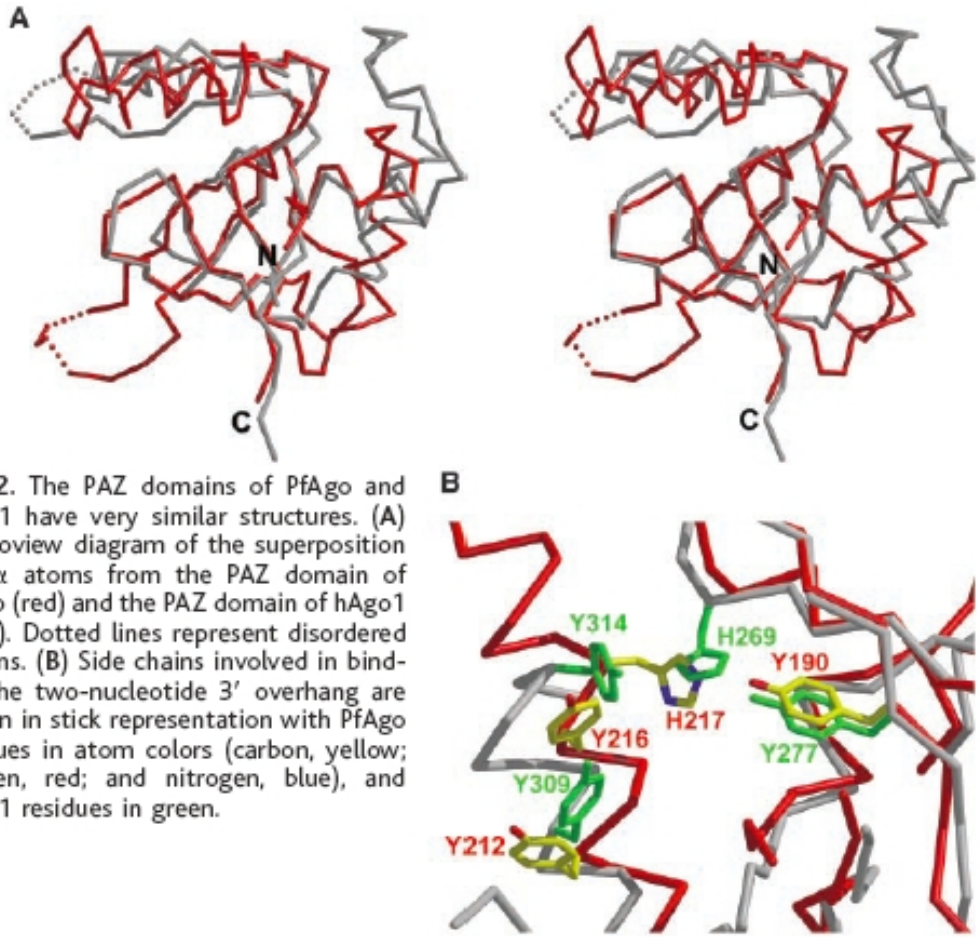

Fig. 2. The PAZ domains of PfAgo and hAgo1 have very similar structures. (**A**) Stereoview diagram of the superposition of Cα atoms from the PAZ domain of PfAgo (red) and the PAZ domain of hAgo1 (gray). Dotted lines represent disordered regions. (**B**) Side chains involved in binding the two-nucleotide 3′ overhang are shown in stick representation with PfAgo residues in atom colors (carbon, yellow; oxygen, red; and nitrogen, blue), and hAgo1 residues in green.

3 SEPTEMBER 2004 VOL 305 SCIENCE

evidenza della conservazione dei residui coinvolti nel legame al 2 nt 3' overhang

il dominio PIWI si ripiega in una struttura simile al dominio dell'RNasi H

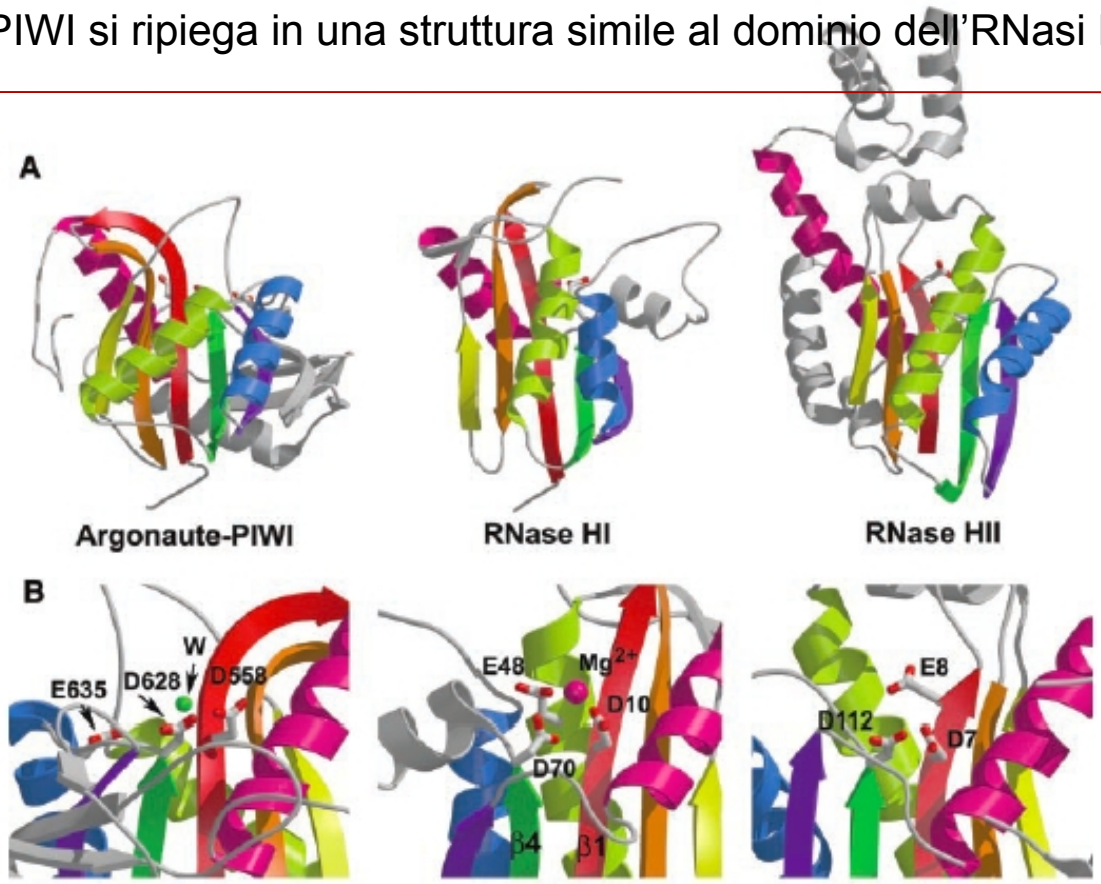

Fig. 3. PIWI is an RNase H domain. (A) Ribbon diagrams of the PIWI domain, *Escherichia coli* RNase HI and *Methanococcus jannaschii* RNase HII. The three structures are shown in a similar view with the secondary structure elements of the canonical RNase H fold in color. Active site residues are shown in stick representation. (B) This view of the active site residues is rotated ~180° about the *y* axis compared with the view in (A). The Mg^{2+} ion in RNase HI is shown as a pink sphere. A strong difference electron density (>4.5σ) found in the active site of PIWI that was assigned as a water molecule is shown as a green sphere. Secondary structural elements of the RNase H fold are colored from red to pink (red, orange, yellow, green, blue, purple, pink) as ordered in the protein sequence.

3 SEPTEMBER 2004 VOL 305 SCIENCE

un solco carico positivamente posizionerebbe il duplex guidaRNA-mRNA al centro del sito catalitico del dominio PIWI

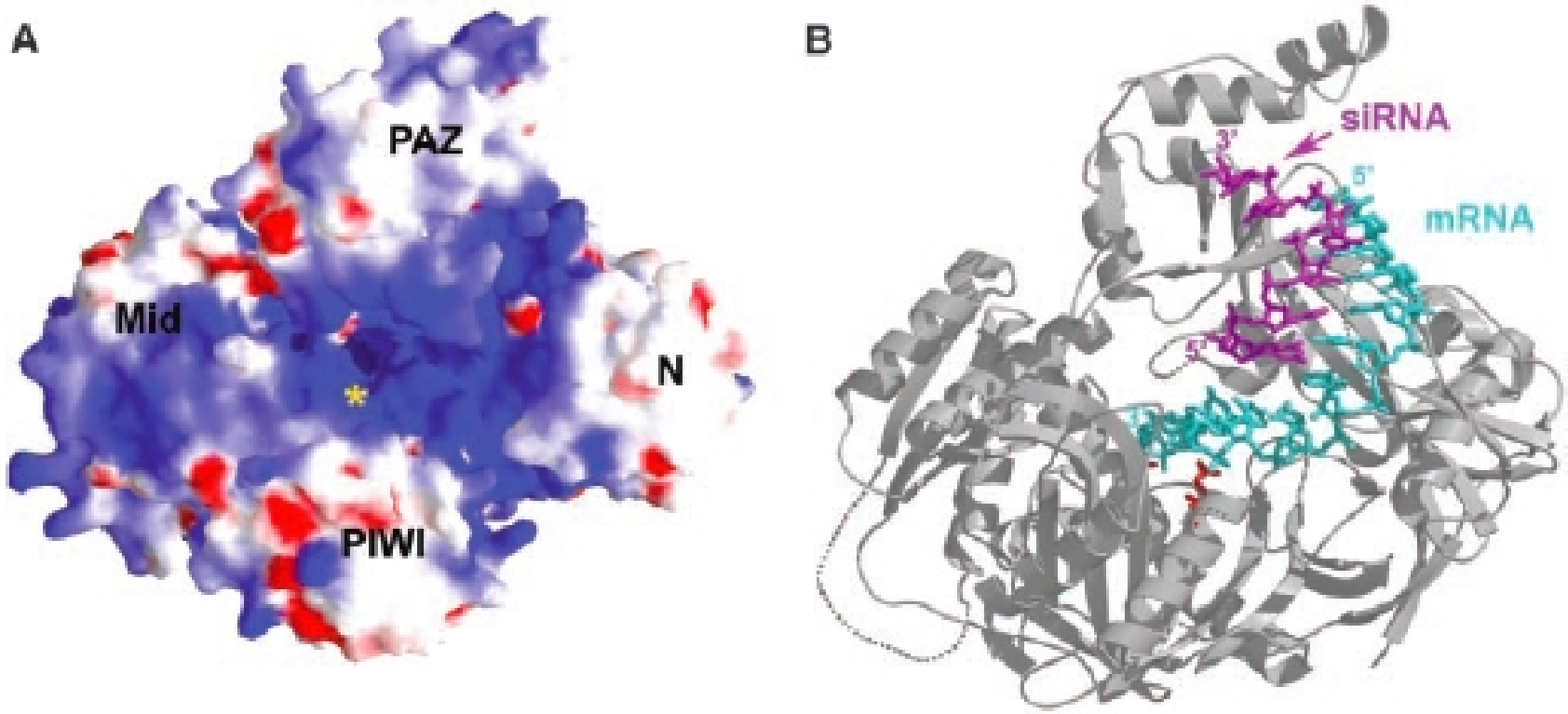

3 SEPTEMBER 2004 VOL 305 SCIENCE

modello proposto per il taglio del mRNA target mediato da siRNA

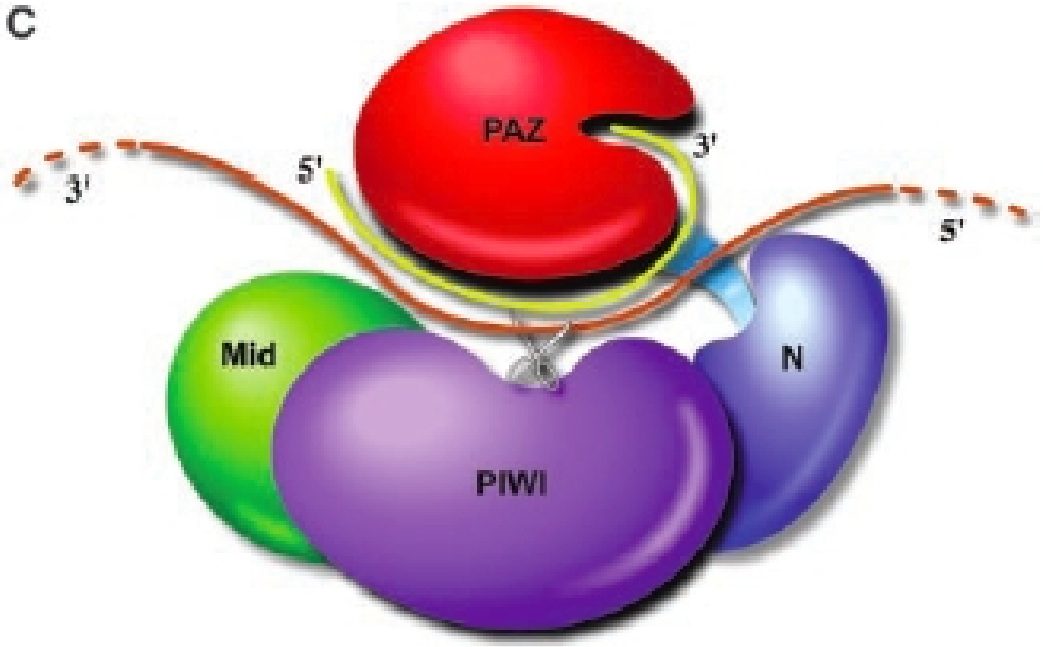

(red). The view is similar to the view in Fig. 1. (C) Schematic depiction of the model for siRNA-guided mRNA cleavage. The domains are colored as in Fig. 1. The siRNA (yellow) binds with its 3′ end in the PAZ cleft and the 5′ is predicted to bind near the other end of the cleft. The mRNA (brown) comes in between the N-terminal and PAZ domains and out between the PAZ and middle domain. The active site in the PIWI domain (shown as scissors) cleaves the mRNA opposite the middle of the siRNA guide.

3 SEPTEMBER 2004 VOL 305 SCIENCE

residui chiave delle proteine Argonaute

triade catalitica (dominio PIWI)

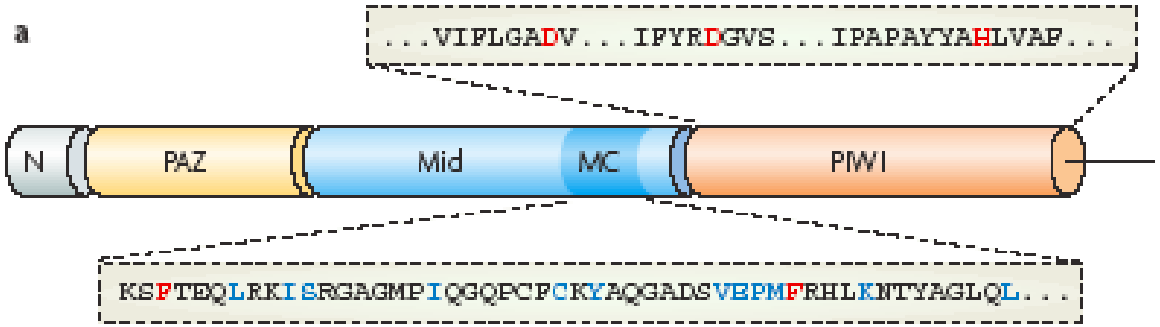

residui coinvolti nel riconoscimento del cappuccio 7'mG ?
(dominio MC-Mid)
omologia con eIF4E (cap binding protein)

dettagli importanti RISC

Proteine della famiglia Argonaute entrano a fare parte del complesso RISC, conferendogli attività di slicer.

Il core funzionale di siRISC nell'uomo è costitutito da DICER, Ago2 e TRBP, e viene caricato con un duplex RNA a complementarietà perfetta (siRNA) o imperfetta (miRNA).

In alcuni organismi siRNA e miRNA, processati da DICER distinte, vengono caricati preferenzialmente su complessi RISC contenti Ago diverse. Il grado di complementarietà del duplex di piccoli RNA sembra giocare un ruolo importante in questa fase di 'sorting'.

Non tutte le Ago complessate a RISC mostrano attività endonucleasica. Nell'uomo per esempio solo Ago2 è attiva come endonucleasi. Molte Ago/PIWI non entrano a fare parte di complessi siRISC o miRISC ma mediano le funzioni associate ai piRNA (vedi oltre), o entrano a fare parte di complessi RISC secondari (secondary Agos, SAGO) coinvolti nell'amplificaizone del silencing (vedi oltre), o mediano i fenomeni di endo-RNAi *(ERGO*-1 in *C. elegans* processa siRNA endogeni).

La catalisi della reazione di taglio mediata da Argonaute è a carico del dominio PIWI e avviene esattamente a 10 nt dal 5' del filamento guida, grazie alla presenza di un solco carico positivamente che può accogliere una elica RNA. Probabilmente diverse Ago si differenziano nella possibilità di accomodare nel solco duplex con differenti conformazioni o geometrie dell'elica.

La scelta del filamento guida dipende in larga misura dalla stabilità termodinamica dei termini 5': il filamento con stabilità termodinamica più bassa al 5' (più facile da 'svolgere') funge da filamento guida

maturazione RISC in seguito alla scelta del filamento guida

in seguito alla scelta del filamento guida, il filamento passeggero deve essere rimosso per poter permettere il riconoscimento del target.

per lungo tempo si è supposto che il filamento passeggero fosse svolto da una attività elicasica ATP-dipendente.

…e invece…

è la stessa attività endonucleasica di Ago2 a tagliare il filamento passeggero (o anti-guida)!

inoltre l'attivtà e la maturazione di RISC sembra essere un processo ATP-indipendente

il taglio del filamento passeggero attiva RISC facilitandone l'assemblaggio su ssRNA messaggeri target.

essendo molte delle Ago associate a miRISC non attive endonucleoliticamente, come si spiega la degradazione del filamento passeggero di miRNA?!

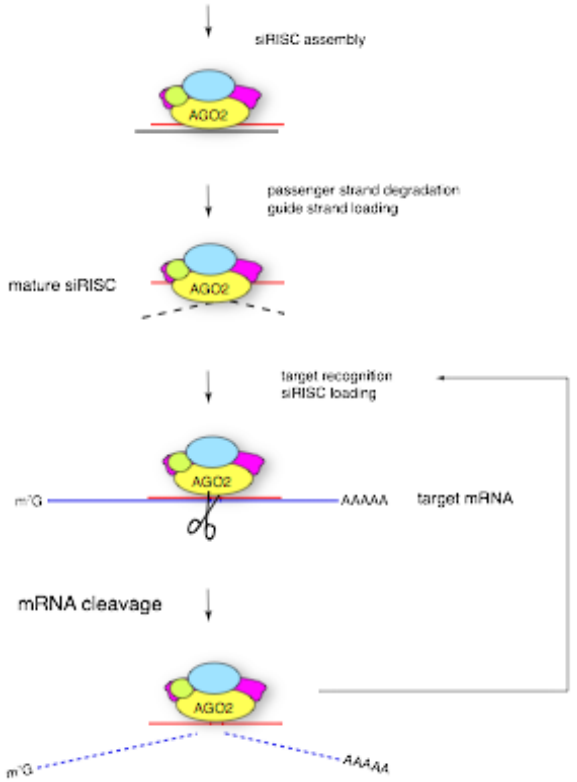

basi molecolari per il riconoscimento del messaggero target da parte di hRISC: l'accessibilità del sito target determina l'efficienza di taglio di RISC

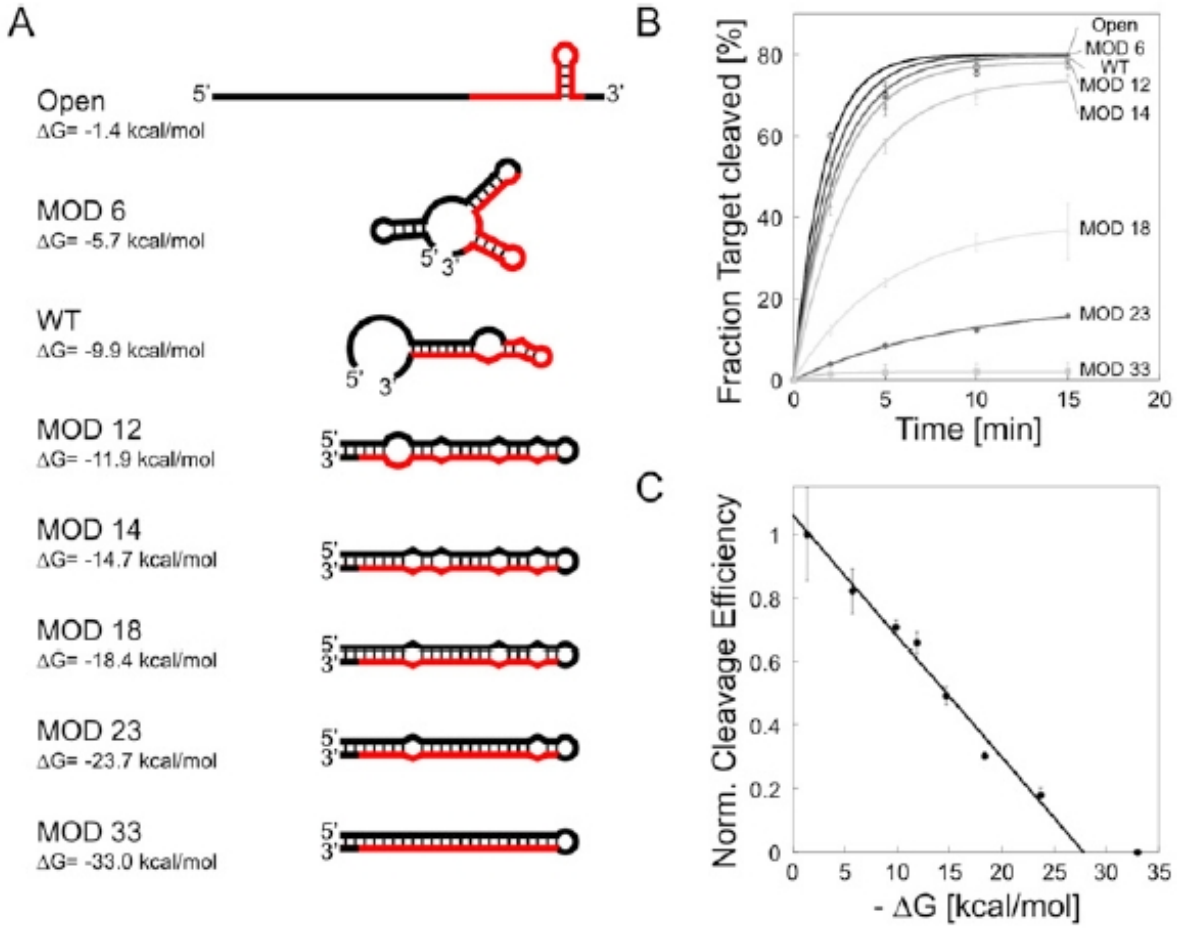

il riconoscimento del target richiede appaiamento delle basi 2-15 del siRNA

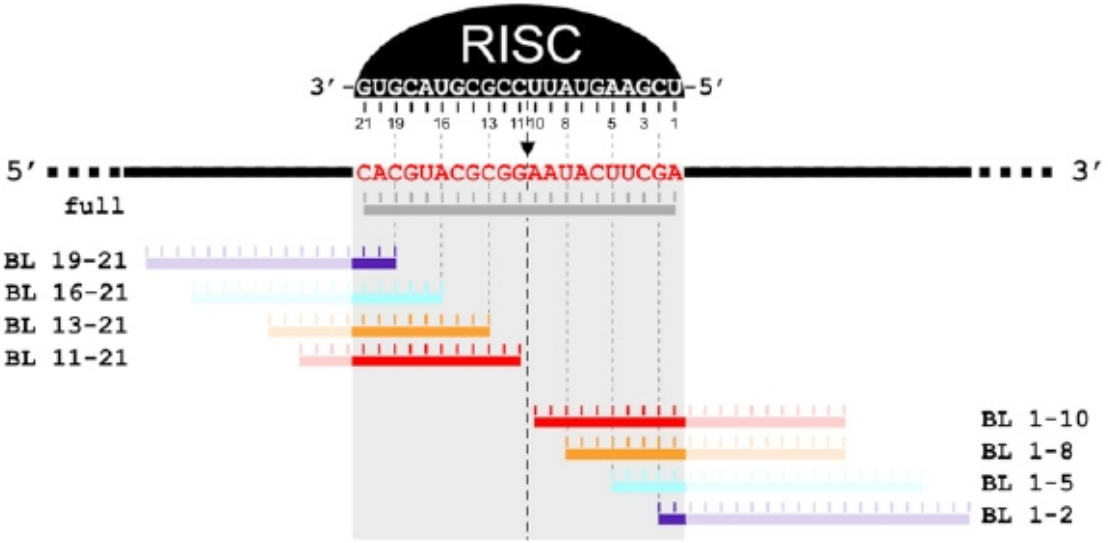

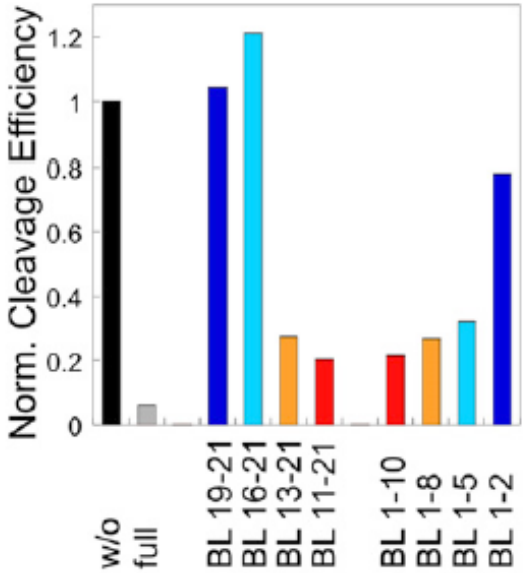

Cell *130*, 101–112, July 13, 2007 ©2007 Elsevier Inc.

appaiamenti imperfetti del 3' promuovono il turnover di RISC

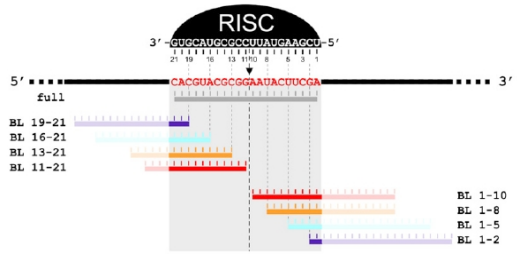

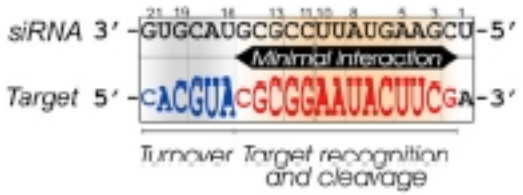

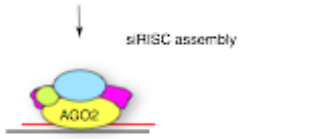

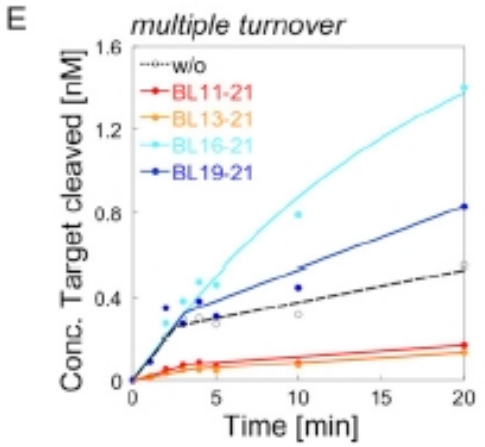

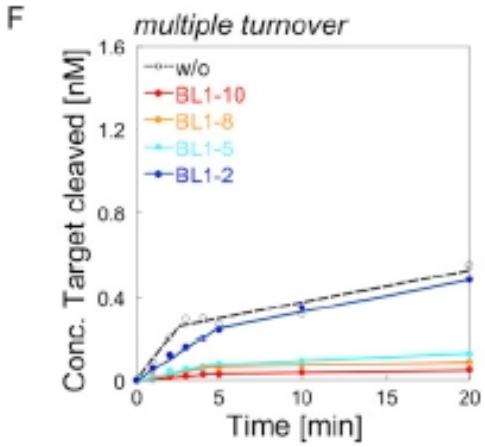

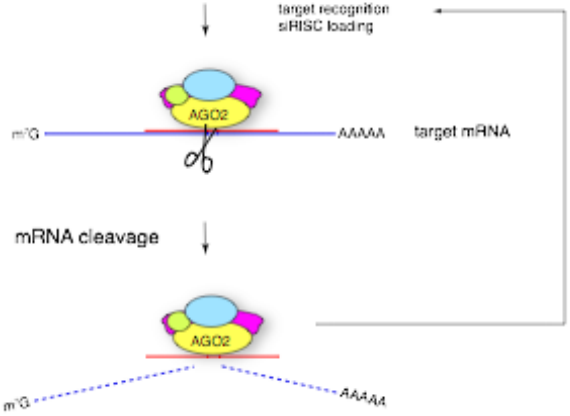

Cell *130*, 101–112, July 13, 2007 ©2007 Elsevier Inc.

RISC interagisce non-specificamente con ssRNA ma non con dsRNA

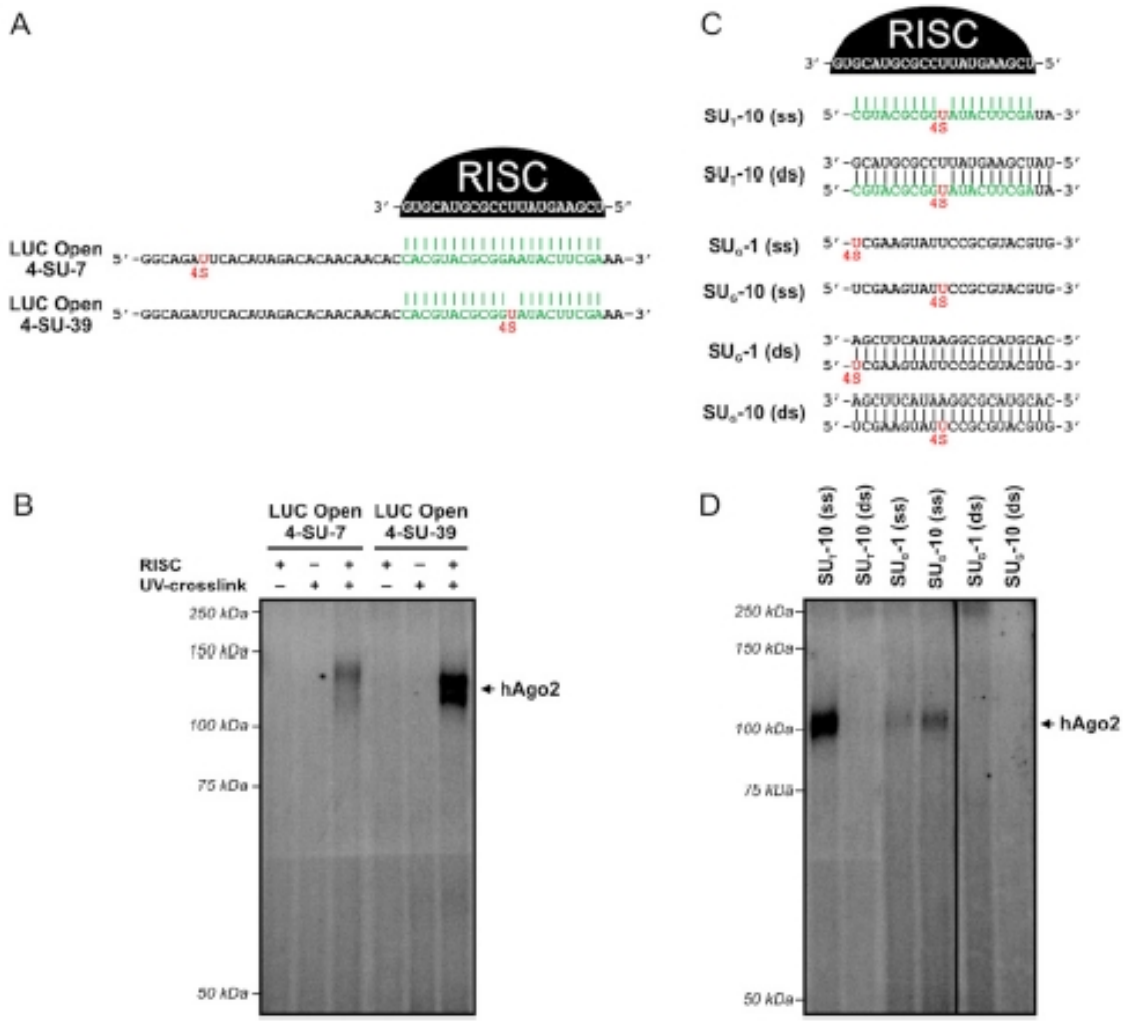

modello proposto per il riconoscimento e taglio di mRNA target mediato da hRISC

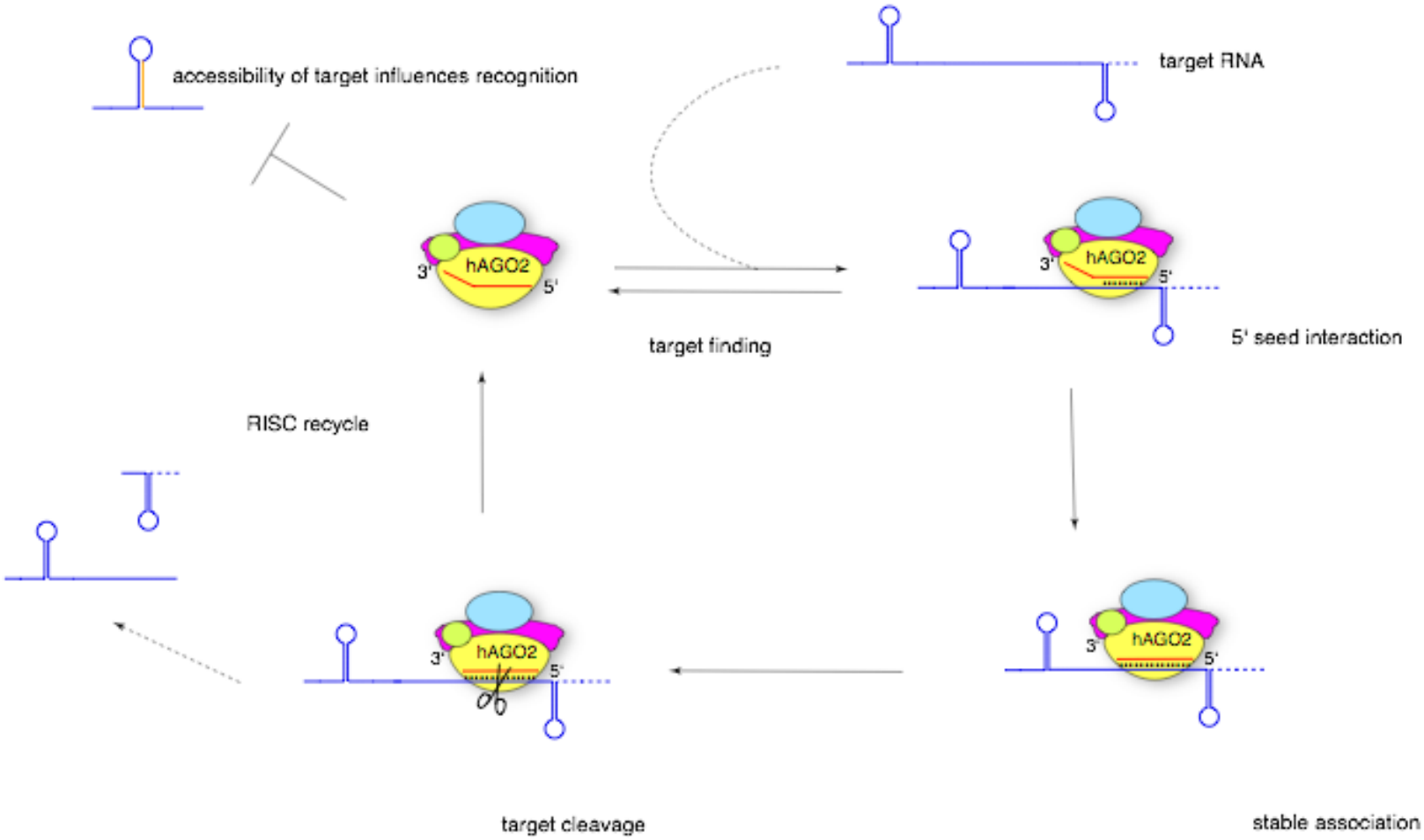

‘stop-motion’ cristallografica di un Ago al lavoro

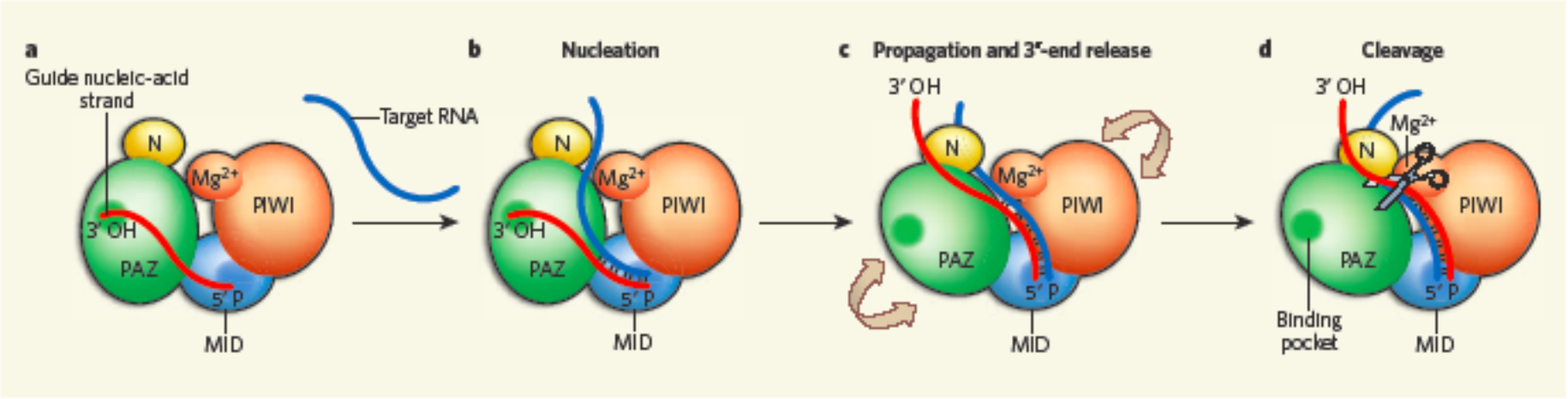

Figure 1 | The Argonaute silencing complex at work. **a**, Argonaute proteins have four domains: the amino-terminal domain (N), PAZ, MID and PIWI. Each Argonaute protein binds to a small nucleic-acid molecule (red; RNA in plants and animals, and DNA in bacteria), which functions as a template for binding to complementary target RNA. The 5′-phosphate (5′ P) end of the guide nucleic acid is anchored in the MID domain, and the 3′-hydroxyl end (3′ OH) is anchored in the PAZ domain. **b**, Structural studies by Wang and colleagues[2] reveal that when the Argonaute complex binds to target RNA, the nucleation step begins with formation of a double helix by base pairing between the guide nucleic acid and the target RNA, commencing at the 5′-phosphate end of the guide strand. **c**, Pivotal movement of the Argonaute protein allows extension of the double helix while the guide DNA is anchored at both ends. The 3′-hydroxyl end of the guide strand is then released from the PAZ domain, allowing its rotation. **d**, This conformational change favours the exact positioning of the target RNA cleavage site close to the Argonaute PIWI domain. Magnesium ions in the PIWI domain facilitate precise cleavage of the target.